



#3

# USE OF ELECTROCHEMILUMINESCENCE FOR VISUALIZING FIELDS OF FLOW

BRADFORD HOWLAND

WALTER H. PITTS

ROBERT C. GESTELAND

Loan Copy

TECHNICAL REPORT 404

SEPTEMBER 21, 1962

Only

MASSACHUSETTS INSTITUTE OF TECHNOLOGY  
RESEARCH LABORATORY OF ELECTRONICS  
CAMBRIDGE, MASSACHUSETTS

The Research Laboratory of Electronics is an interdepartmental laboratory in which faculty members and graduate students from numerous academic departments conduct research.

The research reported in this document was made possible in part by support extended the Massachusetts Institute of Technology, Research Laboratory of Electronics, jointly by the U.S. Army (Signal Corps), the U.S. Navy (Office of Naval Research), and the U.S. Air Force (Office of Scientific Research) under Signal Corps Contract DA36-039-sc-78108, Department of the Army Task 3-99-20-001 and Project 3-99-00-000; and in part by Signal Corps Contract DA-SIG-36-039-61-G14; additional support was furnished by the U.S. Air Force (Aeronautical Systems Division) under Contract AF33(616)-7783; and by the National Institutes of Health (Grant B-2480(C1)).

Reproduction in whole or in part is permitted for any purpose of the United States Government.

MASSACHUSETTS INSTITUTE OF TECHNOLOGY  
RESEARCH LABORATORY OF ELECTRONICS

Technical Report 404

September 21, 1962

USE OF ELECTROCHEMILUMINESCENCE FOR VISUALIZING FIELDS OF FLOW

Bradford Howland, Walter H. Pitts, and Robert C. Gesteland

(Revised manuscript received June 8, 1962)

Abstract

A platinum hydrofoil is immersed in a flowing, alkaline solution containing luminol (5-amino-2,3-dihydro-1,4-phthalazinedione) and  $\text{H}_2\text{O}_2$ . Anodic current, replacing the usual chemical catalysis, generates a bright surface glow with intensity distribution controlled by mass transfer. This displays the flow at the boundary layer without disturbing it. A methanolic solution shows also the flow behind the hydrofoil; the luminescence leaves the anode and extends downstream for a distance determined by the acidity. The subsequent history of parcels of fluid passing by any part of the hydrofoil can thus be traced. Fluid may be recirculated; operation with organic solvents of low kinematic viscosity is possible. Figures illustrate laminar and turbulent boundary layers, various wakes, and vortex streets.

1

2

3

4

5

6

7

8

9

10

## TABLE OF CONTENTS

I. Introduction	1
II. Boundary-Layer Display	3
2.1 The Electrochemical System	3
2.2 Apparatus	5
2.3 Experiments with Circular Flow Chamber	6
2.4 Use of Nonaqueous Solvents and the Heat-Transfer Analogy	9
2.5 Photometric Considerations	16
III. Illumination of Trails and Wakes	20
IV. Summary	24
Appendix Calculation of Exposure for Boundary-Layer Photographs	25
Acknowledgment	27
References	28



## I. INTRODUCTION

Although the study of chemiluminescence — the generation of light by purely chemical means — is a very old one, the consequences of replacing the usual chemical catalysis by an electrical stimulation, while noted previously,<sup>1-3</sup> have not been extensively studied. This is unfortunate, since the phenomenon of electrochemiluminescence, in addition to possessing important technical applications, may yield new clues toward understanding the chemiluminescent process.

We are concerned here with two ways by which electrochemiluminescence may be used to study fluid-flow behaviour. With the first method, a continuous display over the entire surface of a hydrofoil, which shows the state of flow at the boundary layer, is obtained. With the second method, fluid that contacts a hydrofoil is rendered luminous for a time that is sufficient to reveal the structure of the wake or trail. Each of these presentations can be operated continuously in a recirculating flow chamber. With minor exceptions, the disturbance to the phenomenon is negligible. These methods are particularly well suited for studying time-variant flow phenomena, for observing transitions between flow regimes, and in situations in which the inclusion of extraneous substances in the fluid stream, or the apparatus for introducing them, would seriously disturb the flow.

The electrochemical effects on which these methods depend are easily illustrated by the following simple experiment. We prepare an uncatalyzed chemiluminescent solution based on luminol (5-amino-2,3-dihydro-1,4-phthalazinedione) and containing hydrogen peroxide as the oxidizing agent and an alkali to adjust the pH. (Catalysts, such as potassium ferricyanide or sodium hypochlorite, added in small amounts to this solution would release the entire bulk glow in a matter of minutes.) We also add substantial amounts of potassium chloride to increase the conductivity. Into this solution we insert two platinum electrodes of approximately equal area and apply a potential difference of 2 volts. A blue glow, momentarily very bright, will be observed to cover the anode; but it diminishes rapidly in intensity until it is just visible in a darkened room.

The electrode reaction at the anode evidently acts as an effective stimulus for the chemiluminescent glow and leads to rapid exhaustion of the reactants in the vicinity of the surface; the residual glow is determined by the rate of diffusion of fresh reactants thereto. If we now agitate the electrode or stir the fluid, still keeping the voltage applied, the glow at the anode will be re-established, although not with the same initial brightness. The pattern of glow over the surface of the anode reveals the fluid-flow pattern.

Except for the proportioning of the ingredients of the solution, this experiment has only one variable, the applied voltage, which is best specified in terms of the potential difference between the anode and a saturated KCl-calomel electrode located in the solution nearby. If this difference is less than 0.6 volt, the glow pattern is faint and of low contrast and it disappears entirely below 0.3 volt. Good flow patterns are obtained in

the range 0.8-1.2 volts.

If the voltage is still further increased, a second effect, a new surface glow, occurs; it has the appearance of a corona, or thin, glowing halo, covering the anode. This glow does not, however, remain confined to the surface of the anode, but, instead, spills into the fluid at points of flow separation and passes downstream in the form of luminous streamers or a wake of gradually decaying brilliance.

With this simple experiment we are able to illustrate both aspects of the electro-chemiluminescent technique of flow visualization: (a) the surface glow, occurring at low voltage, which reveals effects occurring at the boundary layer, and (b) the volume glow, occurring at higher voltage, which reveals the progress of the fluid subsequent to its passage through the boundary layer.



## II. BOUNDARY-LAYER DISPLAY

### 2.1 THE ELECTROCHEMICAL SYSTEM

A solution that is suitable for showing flow phenomena at the boundary layer of an anodic platinum hydrofoil is given in Table I. This formula provides very nearly the maximum brightness and contrast that are possible if we also require that there be no accumulation of insoluble reaction products and no visible bubbling at the anode. Also to prevent bubbling, we specify that the solution should be degassed; this is easily accomplished by vacuum boiling the solution at room temperature immediately before use. (Evidently a small quantity of oxygen is generated at the anode; this is completely absorbed by the degassed solution in normal operation.) The formula given here has

Table I. Solution for showing boundary-layer patterns.

Substance	Amount	Purpose
1. H <sub>2</sub> O	***	Solvent
2. KCL	1 N	Supporting electrolyte
3. KOH	0.01 N	Adjusts pH
4. H <sub>2</sub> O <sub>2</sub>	5 ml/l of 3 % solution ( $8.5 \times 10^{-4}$ N)	Oxidizing agent
5. Luminol <sup>a</sup>	150 mg/l ( $4.4 \times 10^{-3}$ N)	Chemiluminescent substance
6. EDTA <sup>b</sup>	Trace	Chelating agent
7. Dissolved Air	less than 50 % saturation	To avoid bubbling

<sup>a</sup>Eastman Kodak Company, Luminol = (5-amino-2, 3-dihydro-1, 4-phthalazinedione).

<sup>b</sup>Eastman Kodak Company, EDTA = (Ethylenedinitrile) tetraacetic acid.

been optimized for use in a small flow chamber operating at Reynolds numbers (Re) not exceeding 30,000. At higher Reynolds numbers, flow patterns with this solution have poor contrast; a reduction of the peroxide concentration corrects this difficulty.

Water is here the solvent; it should be distilled, since traces of copper or iron will produce an objectionable bulk glow. The supporting electrolyte is KCl, which also should be very pure since it is added in large amounts. The conductivity provided by this salt causes the voltage drop in the solution to be quite small – commonly a few tenths of a volt in normal operation.

Since luminol is soluble only in alkaline solutions and does not exhibit chemiluminescence below pH 8, it is necessary to make the solution strongly alkaline. The addition of KOH as specified in Table I results in a pH of 11.75. We use less than one-half the amount of luminol that can be dissolved at this pH, since larger amounts often result in an accumulation of insoluble reaction products at the anode. The concentration of  $\text{H}_2\text{O}_2$  strongly affects the intensity and contrast of the glow pattern; amounts larger than specified in Table I will lower the contrast and tend to cause bubbling at the anode.

Changes of relative concentrations of the luminol, hydrogen peroxide, or potassium hydroxide affect, in complex and subtle ways, the behaviour of the electrochemiluminescent system, for example, by altering the shape of the polar light output curve and also the frequency response for electrical modulation of the glow. We do not attempt to delineate the limiting proportions of the reactants which result in satisfactory flow patterns. Small changes of the specified concentrations or alteration of the strength of the supporting electrolyte have little effect on the appearance of the flow patterns. This solution is also insensitive to simultaneous reduction of the concentration of all of the reactants; satisfactory operation, but with reduced light output, is obtained with 1:5 dilution with water or with 1:1 dilution with glycerin.

If a slight bulk glow is exhibited by the solution, it may be eliminated by the addition of a very small quantity of EDTA, a chelating agent that ties up small traces of copper and iron; only a very small amount should be added, however, as this substance has an adverse effect on the reaction. We have so far obtained satisfactory results only with platinum or platinum-plated electrodes. There is a possibility that certain stainless steels could be used if ac is substituted for dc excitation; however, our experience has not been sufficient to permit a recommendation.

The boundary-layer glow pattern requires but a modest current; 3 ma per  $\text{cm}^2$  is typical, but this requirement varies greatly with the flow situation. A variable-voltage, low-resistance, dc power supply that is capable of providing several times this current density is desirable. Still better would be a "potentiostat," a constant-voltage, regulated power supply that uses feedback from a reference electrode to stabilize the anode-to-solution potential.<sup>4</sup> The reference electrode should be located near the anode; the cathode may be located elsewhere, but should have an area at least as great as that of the anode to minimize bubbling at that electrode.

Before operation, the anode must be cleaned; a solution of KOH in methanol has proved quite satisfactory for this purpose. However, if the pattern of glow at the anode still shows irregularities caused by surface effects or if there is bubbling with normal applied voltage — the results of improper cleaning — one should then use electrolytic cleaning. With the fluid in motion, the anode voltage is increased by several volts for a few seconds and some bubbling is produced; an intense trail of glowing fluid results. When this glow has passed into the solution and the bubbles are eliminated, the system should operate normally. Prolonged cleaning is harmful to both the electrodes and the solution and should be avoided.

Several liters of chemiluminescent solution should suffice to display the flow pattern over the surface of a small (one-square-inch) hydrofoil for an hour with little diminution of glow intensity. After several hours it may be necessary to re-evacuate the solution or to replenish the hydrogen peroxide, which tends to bubble out on parts of the apparatus (particularly those made of plastic). Exhaustion of the solution by the electrochemiluminescent reaction is indicated by a brown discoloration and a strong tendency for it to absorb its own light output. The solution also deteriorates, with some change in color, whether it has been used or not; after 12 hours at room temperature it will no longer produce satisfactory flow patterns and should be discarded.

## 2.2 APPARATUS

Our first flow chamber consisted of a beaker; the fluid was moved by a stirring magnet at the bottom. More consistent results have been obtained with the apparatus shown in Fig. 1. Here the fluid is propelled by rotation of the container, a cylindrical glass dish either 7 or 10 inches in diameter, which is filled with two liters of solution. The glass bowl is attached with wax to a pulley mounted on a stainless-steel shaft supported by instrument-quality ball bearings, the assembly being driven by means of assorted pulleys and rubber belts and a variable-speed dc motor. With this arrangement a wide range of Reynolds numbers can be obtained. The hydrofoil is placed near

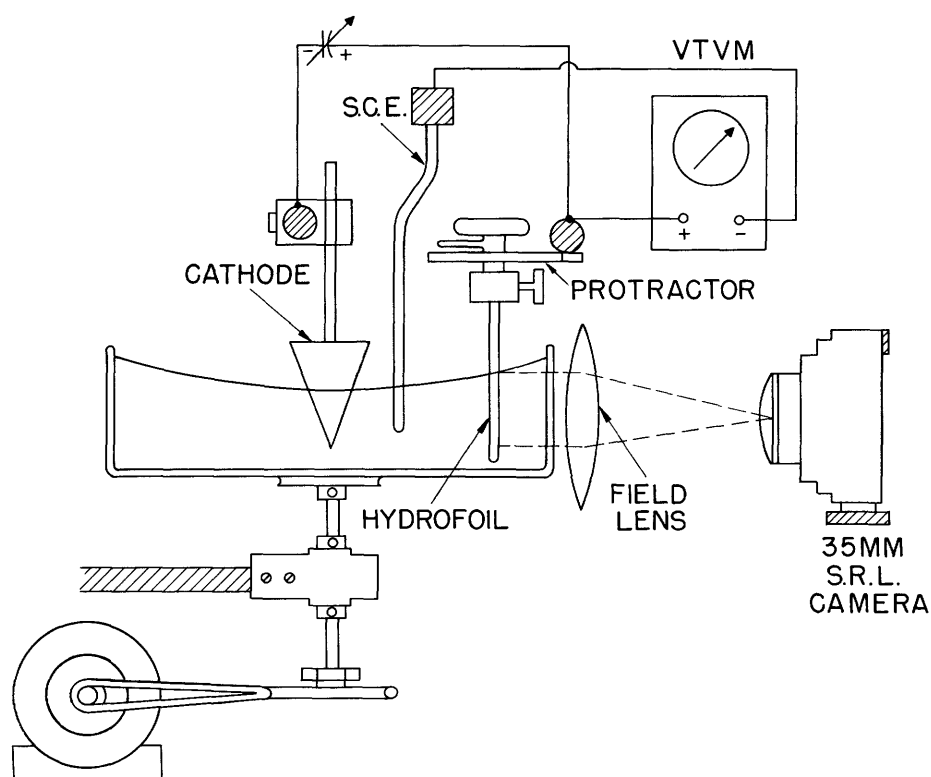


Fig. 1. Circular flow chamber and associated apparatus.

the periphery of the bowl, and provision is made for varying by known amounts its angle of attack relative to the fluid stream. Also included are a tachometer to monitor the speed of the motor, an ammeter to measure the current, and a vacuum-tube voltmeter to measure the potential difference between the solution and the anode.

The pattern of glow was photographed with a 35-mm single-lens-reflex camera using a 50-mm, f1.9 lens, and extension tubes. In Fig. 1 we have placed a field lens directly in front of the test object and have located the camera with its aperture stop at the focus. This arrangement, while not used extensively here, is to be recommended for its antiparallax features.<sup>5</sup> It is equivalent to locating the camera at infinity, since it produces an image that is the true projection of the test object onto a plane (or if viewed from an angle, an isometric projection).

With the flow chamber of Fig. 1 we can demonstrate a number of interesting phenomena of low-speed aerodynamics; for this reason, and because of its simplicity and modest requirement as to volume of chemiluminescent fluid, we believe that this apparatus is particularly well suited for instructional purposes. There are, however, certain disadvantages that are a hindrance in more exacting studies. (a) We are limited to modest Reynolds numbers, approximately 30,000 for the 10-inch bowl, because of centrifugal effects on the fluid; (b) the turbulence introduced into the stream is significant; at large Reynolds numbers it can be detected in the flow pattern on the front surface of cylinders of moderate size; (c) there are optical distortions that preclude accurate measurements of distances about the hydrofoil; and (d) it is difficult to determine the fluid-stream velocity because of the rotational drag exerted by the hydrofoil.

### 2.3 EXPERIMENTS WITH CIRCULAR FLOW CHAMBER

We examined the boundary-layer flow patterns for anodes of a number of simple shapes, including cylinders, spheres, and a flat plate, and for a hydrofoil as a function of Reynolds number. For the cylinder, the flow was normal to the axis. For the flat plate and the hydrofoil, observations were made for different angles of attack and for different Reynolds numbers. The presentation of these results will necessarily be pictorial in nature.

Figure 2 shows a cylinder immersed in the fluid, operating at  $Re = 6000$ ; the flow is from left to right, and the view is normal to both the axis of the cylinder and the direction of flow. (Some ambient light was provided to show the surface of the fluid.) This figure shows clearly the locus of points of flow separation, which appears as a vertical dark line. Farther to the rear, we observe the interaction of the turbulent wake with the surface of the cylinder; a motion-picture film strip would reveal the constantly changing nature of these disturbances. This pattern is characteristic of the behaviour of cylinders over a range of Reynolds numbers; however, both the granularity of the turbulence and the average surface brightness

increase with velocity of flow. The exposure for this picture, which was minimal, was f3.5 at 1/10 sec; we used improved Tri-X film, developed to ASA 1000. These data define the exposure requirements and specify, albeit indirectly, the absolute brightness of the electrochemiluminescent glow.



Fig. 2. Boundary-layer flow pattern for cylinder with  $Re \approx 6000$ . Some ambient light was provided. Fluid flow is from left to right.

Figure 3 shows various patterns with fluid flowing from left to right past a square plate supported at the top by a slotted, cylindrical nylon rod. In Fig. 3a the angle of attack is a few degrees negative; that is, the flow impinges on the surface facing the camera. The flow here is laminar, with some interference effects caused by the supporting rod. This pattern changes little with Reynolds number. Reversal of the sign of the angle of attack results in the pattern of Fig. 3b, for which  $Re = 22,500$ . We note that separation of flow takes place at or very near the leading edge; farther to the rear the disturbances caused by the interaction of the turbulent wake with the surface of the plate are prominent. Motion pictures would indicate the changing nature of these disturbances and their directions and rates of propagation over the surface, which are (fortunately for the photographer) surprisingly slow compared with the velocity of the fluid a short distance from the surface of the plate. Two strong vortices starting at the front corners are evident; these give rise to the brightest glow and are quite stable;

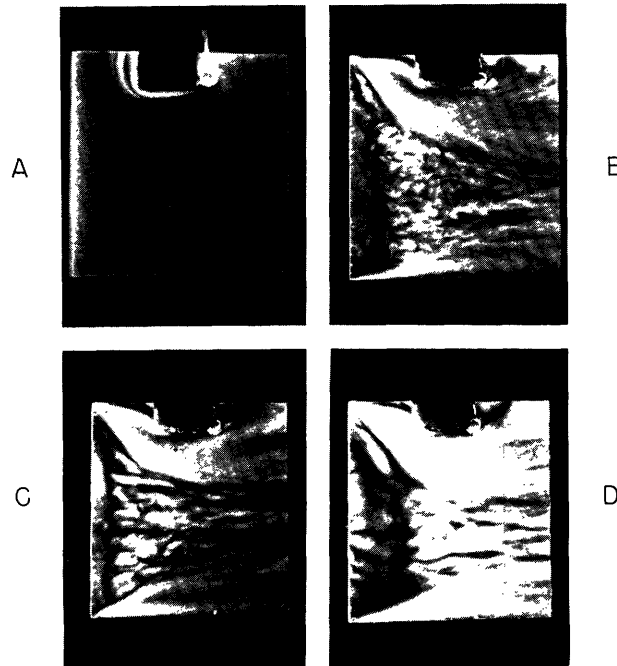


Fig. 3. Patterns of flow past square plate for different Reynolds numbers: (a) laminar flow,  $Re = 10,000$ ; (b) separated flow,  $Re = 22,500$ ; (c) separated flow,  $Re = 10,000$ ; and (d) separated flow,  $Re = 2500$ .

that is, they do not move about.

Changing the Reynolds number alters the flow patterns in an interesting way. Figure 3c shows the effect of reducing the fluid velocity by a factor of 2.25 and keeping the angle of attack the same as in Fig. 3b. Figure 3d shows the effect of reducing the fluid velocity by an additional factor of 4. The predominant effect here is a decrease in the granularity of the turbulent disturbances; at a sufficiently low speed, the time variations in the pattern disappear entirely.

We next consider the effect of varying the angle of attack. This is illustrated in Fig. 4 for an imperfectly shaped, blunt-nose hydrofoil operating at  $Re = 9000$ . Figure 4a shows a laminar flow situation. (The alteration in shading which occurs two-thirds of the way to the rear is caused by an abrupt change in the taper of the cross section of the hydrofoil.) In Fig. 4b we have increased the angle of attack, and here we note the beginning of disturbances that have been identified as transitional streamers. These are stable in location and are associated with foreign inclusions, that is, small hairs or particles of dust that accumulate at the leading edge. As we increase the angle of attack we have a further development of these factors (Fig. 4c), and, finally, in Fig. 4d a fully separated flow, together with prominent vortices at top and bottom.

The patterns of flow past cylinders are discussed in detail in section 2.4. The patterns of flow past spheres are qualitatively similar to those for cylinders. Because of the limitations of our flow chamber, we are at present unable to show the classical

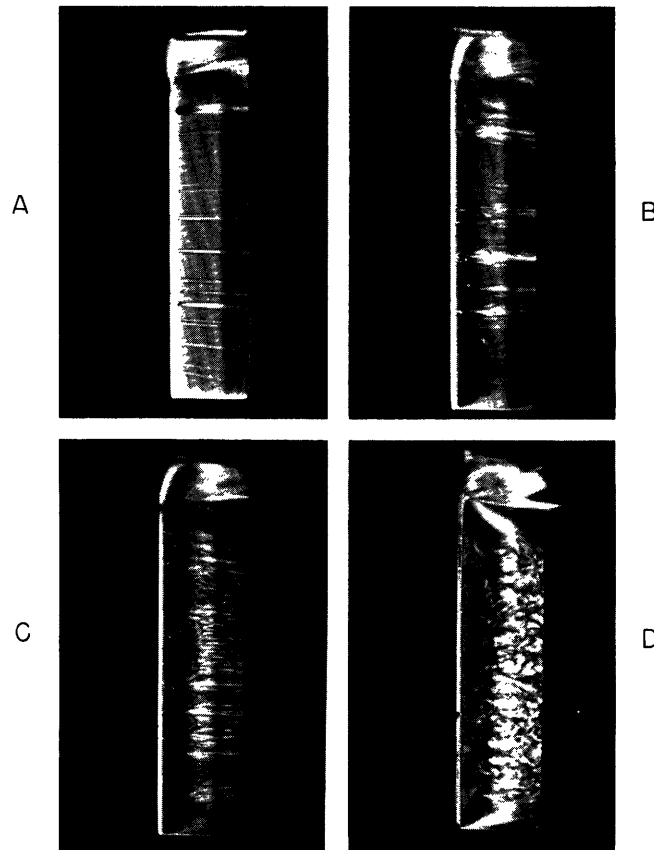


Fig. 4. Flow past hydrofoil for  $Re = 9000$  with various angles of attack producing (a) essentially laminar flow at  $\theta = -5^\circ$ ; (b) transitional streamers at  $\theta = +1^\circ$ ; (c) more extensive development of streamers at  $\theta = +2^\circ$ ; and (d) fully separated flow at  $\theta = +8^\circ$ .

transition from laminar to turbulent boundary layer which occurs with these shapes in the range  $Re = 10^5$  to  $Re = 10^6$ . However, because of the analogy between mass and heat transfer, it is quite unlikely that any such transition involving large changes in the heat-transfer coefficient would be unobservable with this flow-visualization technique.

#### 2.4 USE OF NONAQUEOUS SOLVENTS AND THE HEAT-TRANSFER ANALOGY

The electrochemiluminescent boundary-layer display operates as well with water-glycerin mixtures as with water itself. If we increase both the viscosity of the mixture and the velocity of flow by the same factor, then the Reynolds number, and thus the pattern of flow, will remain unchanged; the net result will be a speeding up of the time scale of the hydrodynamic phenomena. Such an artifice may prove to be useful for the visual observation of phenomena occurring at very low Reynolds numbers.

The possibility of operating with solvents having lower kinematic viscosity than water is of greater importance for several reasons. (a) The time scale of events will be slowed down to permit longer photographic exposures; (b) the pumping power

required to generate a flow of given  $Re$  will be reduced; (c) for the same flow velocity (the limiting factor in our circular flow chamber) we can attain increased Reynolds numbers; and, finally, (d) a more subtle consequence of choosing a solvent of low viscosity relates to the analogy between mass and heat transfers. These processes are governed by dimensionless parameters – the Schmidt number ( $Sc$ ) and the Prandtl number ( $Pr$ ), the ratios of kinematic viscosity to chemical and thermal diffusivities, respectively. For water, there is considerable disparity between these factors, since  $Sc \approx 1000$  and  $Pr \approx 10$ . If we are to simulate heat-transfer problems exactly with our chemiluminescent system, we require that the Schmidt number for the chemiluminescent solution equals the Prandtl number of the heat-transfer medium.

The importance of the use of such analogue methods has already been outlined by Frank-Kamenetskii,<sup>6</sup> who used the kinetics of dissolution of substances in aqueous solutions to simulate heat transfer in viscous media, and also, incidentally, to obtain information as to the behaviour of the laminar sublayer. We are suggesting the possibility of using the electrochemiluminescent reaction, operating in a nonaqueous solvent of low viscosity, to simulate heat transfer in not-so-viscous media. With this method, the total light output would correspond to the rate of heat transfer, and the brightness of a given region would indicate the instantaneous value of the local Nusselt number. The pattern of glow would thus display the heat-transfer coefficients at all points of the surface as a function of time; this information is difficult to obtain with other experimental techniques.

These considerations prompt us to see how far we can reduce the Schmidt number of our chemiluminescent solution by proper choice of solvent, temperature, and so forth, our aim being to approximate the Prandtl numbers of commonly used heat-transfer media. The situation is made more hopeful by the fact that a decrease in the viscosity of a fluid causes an increase in chemical diffusivity; the ratio is affected doubly. In Table II we have listed various promising nonaqueous solvents, together with their kinematic viscosities,  $\nu$ , and estimates of their Schmidt numbers relative to that of water. (Since we do not know if it is the diffusion of luminol, peroxide, some intermediate ion, or a combination of these factors which limits the rate of the reaction, we cannot assign an absolute value to the Schmidt number. There is also the possibility that the reaction is not a simple, first-order one, and that no analogue with heat transfer exists.) Each of these solvents with appropriate additives will exhibit substantial conductivity. Solubility considerations will dictate the choice of supporting electrolyte, alkali, and perhaps also the chemiluminescent substance.

We have so far been able to generate recognizable flow patterns with the following solvents: (a) water, (b) water-glycerin, (c) methanol, by using luminol, together with tetramethylammonium chloride and hydroxide, as salt and base, respectively, (d) acetone, by using luminol, piperidine perchlorate, and piperidine, and (e) pyridine, by using violanthrone in place of luminol, which gives a brilliant red glow pattern. It is expected that similar success can be achieved with the other solvents listed in



Table II. Kinematic viscosities and relative Schmidt numbers for various solvents.

No.	Solvent	Temperature (°C)	$\nu$ Centipoises	Schmidt Number Relative to H <sub>2</sub> O
1	Water <sup>a</sup>	20	1.00	1.00
2	Water-Glycerin, <sup>a</sup> 1:1	20	6.0	36.2
3	Pyridine <sup>a</sup>	20	1.01	0.82
4	Methanol <sup>a</sup>	20	0.75	0.42
5	Acetone <sup>a</sup>	20	0.418	0.16
6	Ether	20	0.327	0.105
		100	0.17	0.029
7	Liquid SO <sub>2</sub>	0	0.27	0.145
8	Liquid NH <sub>3</sub>	-33.5	0.39	0.130

<sup>a</sup>Flow patterns have been obtained with these solvents.

Table II. It is likely that certain of these variant electrochemiluminescent systems may have advantages over the aqueous solution. We note in particular that the methanolic solution will operate over a very wide temperature range, -35°C to +75°C, and that it has very little tendency to produce bubbles at the anode, even with large degrees of air saturation.

The analogy between heat transfer and mass transfer, insofar as it can be related to the present experiments, should provide us with a valuable quantitative interpretation of our flow pictures. Our knowledge of the electrochemiluminescent process is, however, insufficient to predict, for a given voltage, pH, and proportioning of the reactants, the extent to which mass-transfer effects alone determine the intensity of the electrochemiluminescent glow. That the proper adjustment of these parameters is of critical importance for the success of such an analogy is obvious, since certain restrictions on the composition of the solution are necessary in order to obtain any flow pattern. Also, since the contrast of the pattern of glow is a function of the voltage, strict proportionality between the intensity of surface glow and the corresponding rates of mass and heat transfer everywhere on the surface of the electrode cannot obtain for every voltage for which a flow pattern is evident.

To determine which combination of these parameters (that is, voltage, pH, and concentration of reactants) favors the heat-transfer analogy, we have performed the following simple experiment: Cylinders of the same length and differing diameters were similarly located in the flow chamber, and the total light output from each was measured

as a function of applied voltage and Reynolds number. (The total light was measured by the indirect method described in section 2.5.)

If the intensity of the chemiluminescent glow is limited by the reaction kinetics at the surface, we would expect that those electrodes having the greatest surface area would produce the greatest light output. If, on the other hand, the glow intensity is governed by mass transfer, the light output should be independent of the diameter of the cylinder for the same Reynolds number. This independence is a consequence of the dimensional law governing mass- and heat-transfer processes, which states that the diffusion gradient and, thus, the surface brightness vary inversely with radius; the product of average surface brightness and area is thus independent of radius. The data for our standard solution, with  $E = 0.9$  volt, are given in Fig. 5. For this plot, correction was made for the reduction in fluid velocity which was caused by drag. Within the accuracy of these measurements, the independence of the light output with diameter is substantiated. The variation of total light output with Reynolds number is also in agreement with the published data of McAdams<sup>7</sup> for the corresponding heat-transfer situation ( $Pr \approx 400$ ).

It is apparent that over a considerable range of surface brightness these photometric data are consistent with the assumption that the reaction is controlled by mass transfer

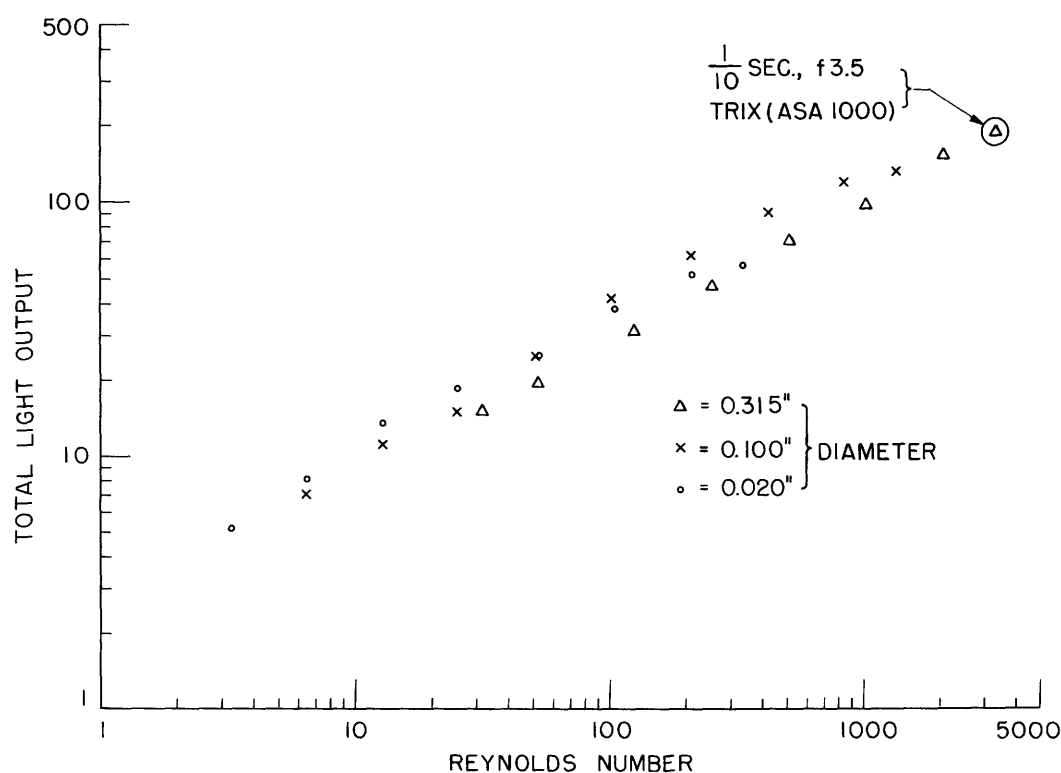


Fig. 5. Total light outputs from cylinders of same length and different diameters, as a function of Reynolds number. (Standard solution,  $E = 0.9$  vdc.)

and is limited only in small part, if at all, by reaction kinetics at the surface. (For proof that the electrochemiluminescent reaction does take place at or very near the surface, see sec. 2.5.) The choice of voltage and composition of solution is quite specific for this result; changes in either the pH or the concentration of peroxide will result in differences in the light outputs from the various cylinders for the same Reynolds number.

A more detailed experiment is one that compares the time-averaged brightness distribution of flow with measurements of the local Nusselt number for different sectors of a cylinder. Figure 6 gives heat-transfer data of Eckert and Soehngen<sup>8</sup> for the flow

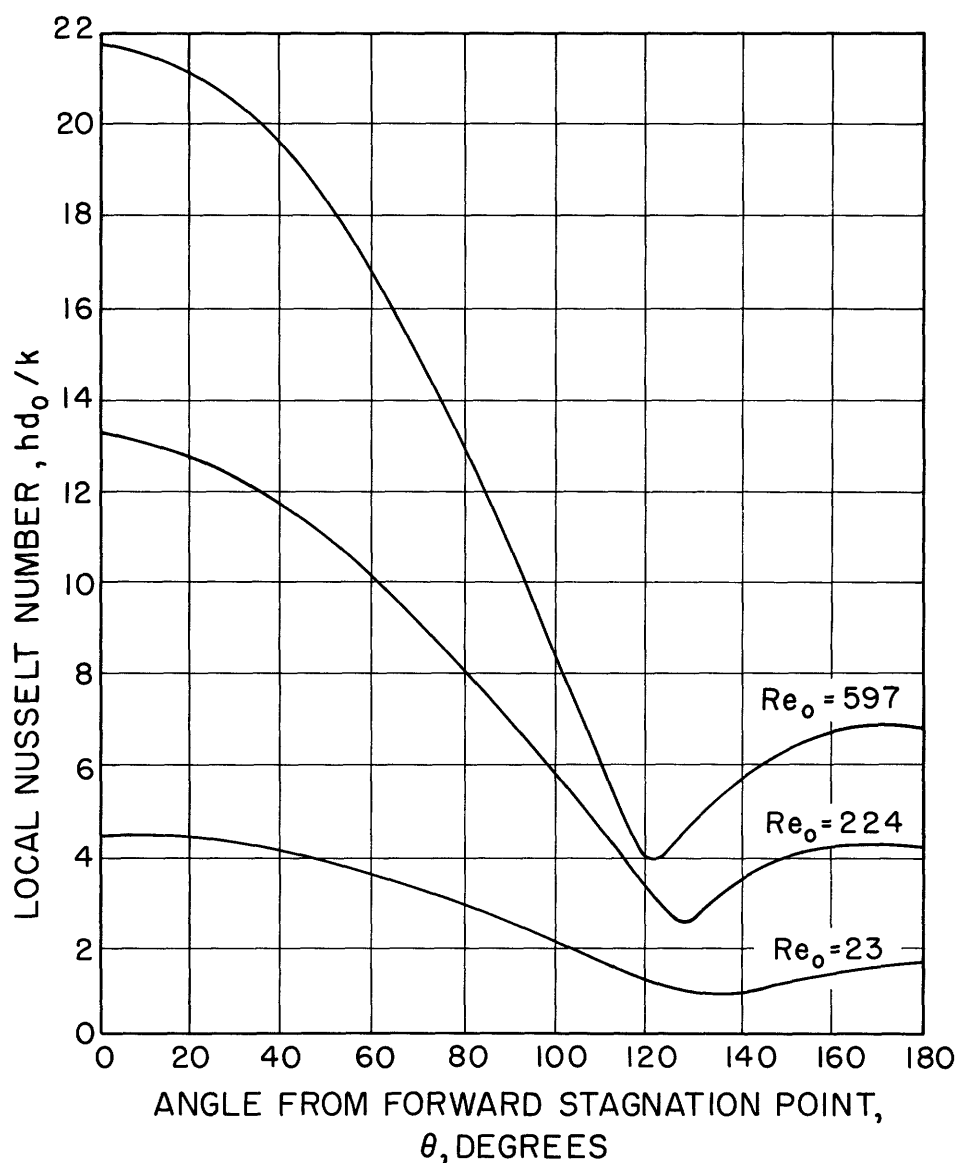


Fig. 6. Local Nusselt numbers for the flow of air past cylinders at low Reynolds numbers. (Based on a figure of E. R. G. Eckert and E. Soehngen, Trans. Am. Soc. Mech. Engrs. 74, 343 (1952).)

of air past a heated cylinder at low Reynolds numbers which were obtained with interferometric measurements. This is to be compared with the set of photographs of flow past frusta of cones shown in Fig. 7, spanning the same range of Reynolds numbers. (These pictures were taken from a direction approximately normal to the direction of flow.) The dark lines that indicate flow separation are in all cases, particularly with overexposure, clearly defined. Their location is seen to correspond to that of the minima in the heat-transfer coefficients; in both cases the location moves to the rear with decreasing Reynolds numbers. This qualitative agreement is encouraging, since it indicates that the disturbance to the flow which is caused by the electrochemical reaction is either very small or zero over this range of Reynolds numbers.

The quantitative interpretation of the photographs of Fig. 7 is subject to two difficulties. (a) Since we cannot observe the flow pattern on the reverse side of the cylinder or cone, we cannot locate accurately the line of separation with respect to the forward stagnation point (the axis of symmetry). (b) Quantitative assessment

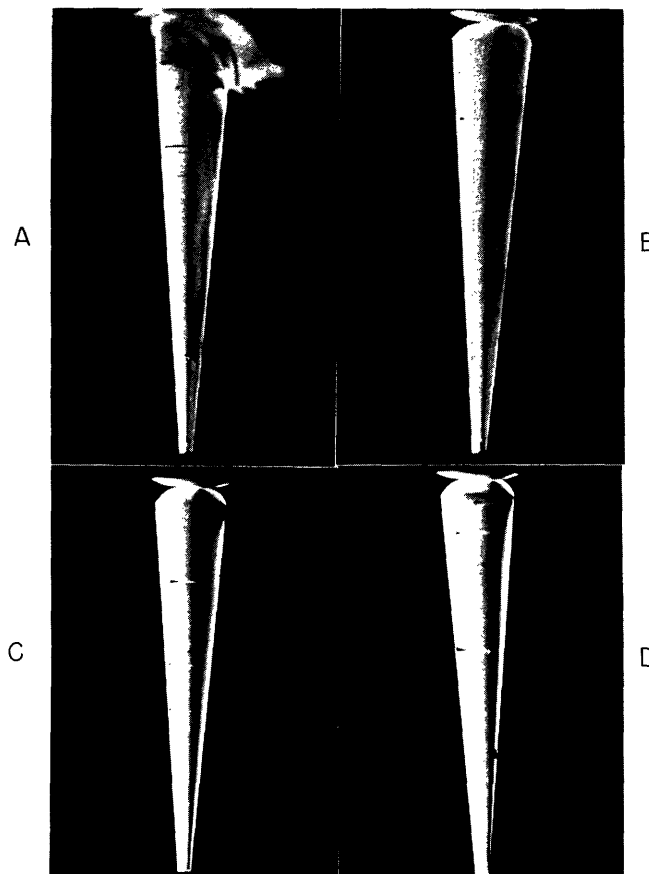


Fig. 7. Pattern of flow past frusta of cones, showing lines of separation for various ranges of Reynolds numbers. (a)  $Re = 4800-800$ ; (b)  $Re = 1200-200$ ; (c)  $Re = 200-33$ , and (d)  $Re = 60-10$ .

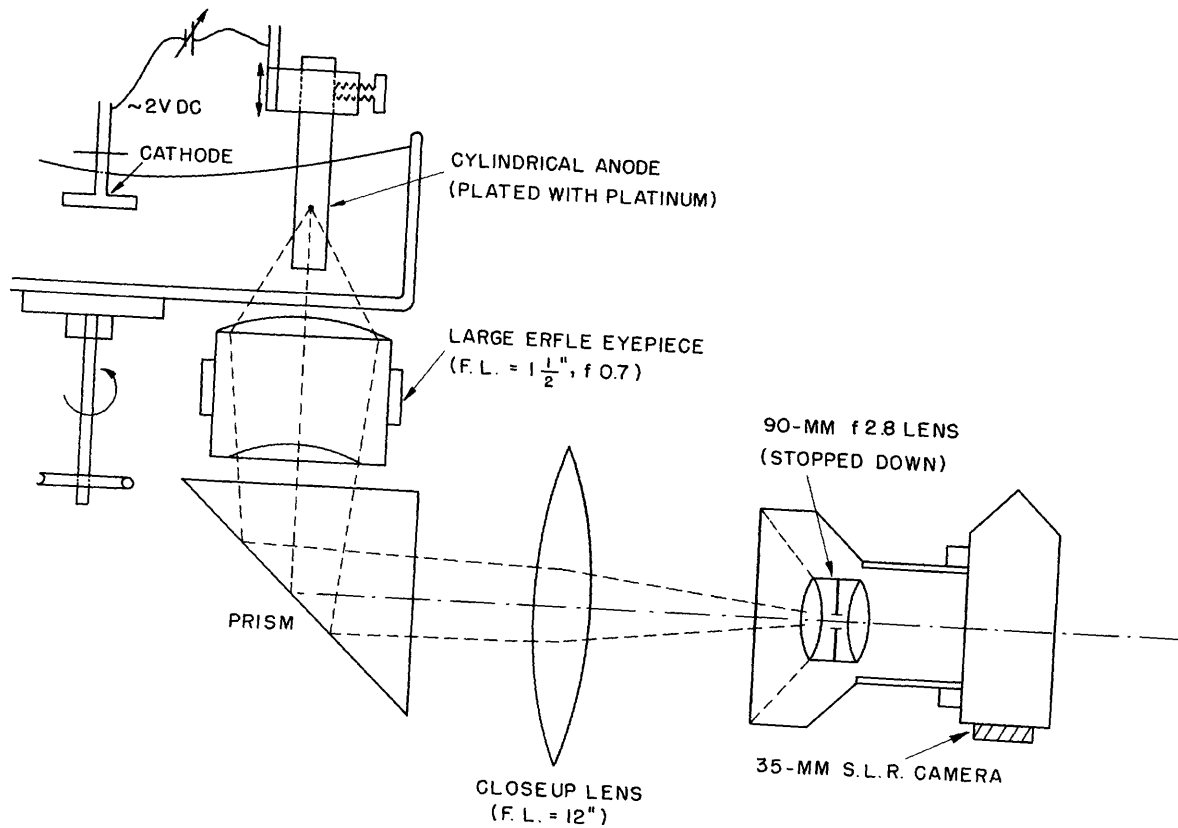


Fig. 8. Optical system for viewing pattern of glow about cylinder with negative parallax distortion.

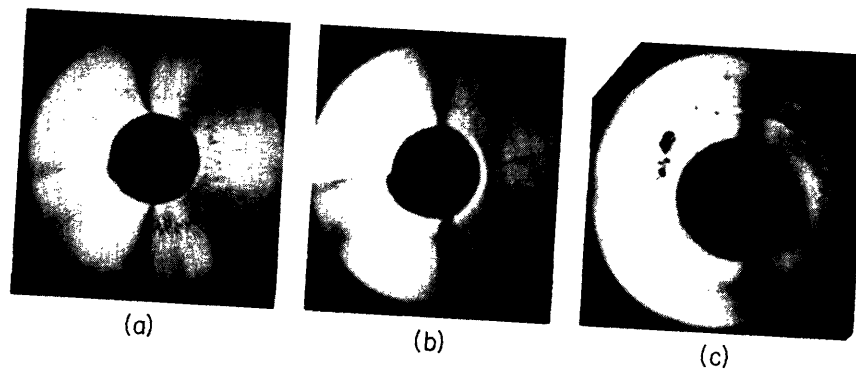


Fig. 9. Flow pattern about cylinder viewed axially with orthoscopic projection (negative parallax distortion). (a)  $Re = 6000$ ; (b)  $Re = 650$ ; (c)  $Re = 70$ . Flow is from left to right.

of the intensity of glow is complicated by the fact that the apparent brightness varies with angle of view (see sec. 2.5).

An improved optical system that overcomes these limitations is shown in Fig. 8. Here the surface of the cylinder is viewed through a lens of wide aperture and short focal length, which is located coaxial with the cylinder and immediately below it.

Objects viewed from a distance through such a highly convergent lens system exhibit orthoscopic perspective (negative parallax distortion); that is, those parts of the object which are nearest the observer appear smallest, while those parts farthest away are imaged with the largest scale of magnification.<sup>9</sup> The effect is to transform a cube into a pyramid (with a flat top), or a cylinder into a frustum of a cone.

With this artifice we are able to photograph the entire pattern of glow about a cylinder without prejudice as to direction of view. Figure 9a shows such a pattern of glow for  $Re = 6000$ , Fig. 9b for  $Re = 650$ , and Fig. 9c for  $Re = 70$ . Note that separation occurs slightly forward of center at the highest Reynolds number, as expected — this was not evident from the photograph of Fig. 7a. Sensitometric interpretation of these or similar data will permit a detailed quantitative comparison of the intensity of glow with heat-transfer data for the analogous flow situation.

## 2.5 PHOTOMETRIC CONSIDERATIONS

The spectrum of the electrochemiluminescent glow appears to be identical to the chemiluminescent glow of luminol.<sup>2</sup> We have also measured the frequency response with which the glow can be electrically modulated. Preliminary results with our standard solution and a 1-mil platinum wire anode show that this response is down 50 per cent at a frequency of 35 kcps; with a flat-plate electrode, however, it is not possible to modulate the glow at rates greater than a few hundred cycles per second. The difference is evidently caused by the effects of polarization capacitance, which is known to be of greater consequence with large electrodes.

Another characteristic of the electrochemiluminescent glow that is of interest is the polar intensity distribution of emitted light; the shape of this curve is closely related to the mechanism of light production. For measurements of this effect, a flat-plate electrode was located at the center of our circular flow chamber. An arrangement of baffle plates sufficed to cause a laminar flow past this anode when the bowl was rotated as in normal operation. The light intensity was measured with a shrouded phototube, located at a distance, which was attached to an arm that moved in a circular arc about the bowl.

Measurements of the electrochemiluminescent glow at the platinum anode, with a solution similar to our standard solution but of reduced alkalinity ( $pH = 11.3$ ), indicated a very simple result: The light output from the plate, as measured by the phototube, was substantially constant throughout a  $174^\circ$  arc, corresponding to  $|\beta| < 87^\circ$ , where  $\beta$  is the angle of view measured from the normal. The surface brightness, which determines photographic exposure and which is proportional to the total light received by the phototube divided by the projected area of the plate, will thus vary as  $\sec \beta$ . The brightness of the plate will thus appear to be least when viewed at normal incidence and greatest when viewed with near-grazing incidence.

This result is consistent with the following simple mechanism of light production: At the surface of the anode, catalysts are assumed to be produced by an electrochemical

reaction involving the decomposition of the peroxide. These catalysts diffuse only a short distance into the solution (too small to be visible in our flow pictures) where they give rise to a chemiluminescent glow. Since the contributions of the molecules in this thin glowing layer are, on the average, nonspecific as to direction, the total light output is essentially constant as long as the surface is in view of the phototube.

Measurements with our more alkaline, standard solution ( $\text{pH} = 11.75$ ) indicate a more complex behaviour. In Fig. 10 the surface brightness and the total light output from a plate of unit area are plotted for both polarizations as a function of angle. Examination of these data reveals the following points of interest: (a) For  $|\beta| < 30^\circ$ , the total light output is essentially constant. (b) If one selects the component of light polarized parallel to the surface, then the total light will be substantially constant for all  $|\beta| < 70^\circ$ . (c) The measured curve of total light output for  $|\beta| > 30^\circ$  is inconsistent with the simple mechanism of light production given above. (d) For  $\beta = 75^\circ$ , the polarization of the emitted light is in excess of that which can be explained by differential reflection at the surface of the platinum; the ratio of intensities of the two components here is 1.62:1 rather than 1.33:1 and can be, in fact, still greater if the solution is made more alkaline. These two points are strong indirect evidence that the glow is generated very close to the reflecting surface, the increased polarization and altered angular distribution resulting from interference between the direct and reflected rays. Since the spectrum of the glow is a rather broad one, at least  $600 \text{ \AA}$  wide, such an effect could occur only if the light generation took place within a few wavelengths of the surface. The separation between the glowing molecules and their images is evidently still further reduced if the solution is made more alkaline, and thus a reduction of the mean lifetime of the catalyzing agent is indicated. This result is consistent with the observation that the frequency response increases with degree of alkalinity.

Knowledge of the polar-brightness distribution is of practical importance, since it affects the interpretation of our flow pictures. For all cases other than that of a flat hydrofoil, a quantitative interpretation of the light intensities in the glow pattern must take into account the shape of the hydrofoil. We have already shown pictures in which such distortions are of consequence; the brightness of the front surface of the hydrofoil shown in Fig. 4 is certainly exaggerated by this effect. Similarly, in Fig. 9 the central areas corresponding to the end of the cylinder, which is viewed here at normal incidence, appear very dark in comparison with the outer surface of the cylinder, which is viewed at grazing incidence.

For certain purposes this same polar-light distribution may be advantageous; in particular, it makes possible a simple method of estimating the total or surface-integrated light output from a hydrofoil. The curves of Fig. 8 show that, with little error, the light received by a photocell at a great distance from a unit area of surface will be sensibly constant for  $\beta < 30^\circ$ . If the hydrofoil is a cylinder, or other such extension of a two-dimensional figure, the inclinations of the surface to the photocell will be predominantly in one plane, and we may extend the limit to  $\beta < 75^\circ$  by selecting only

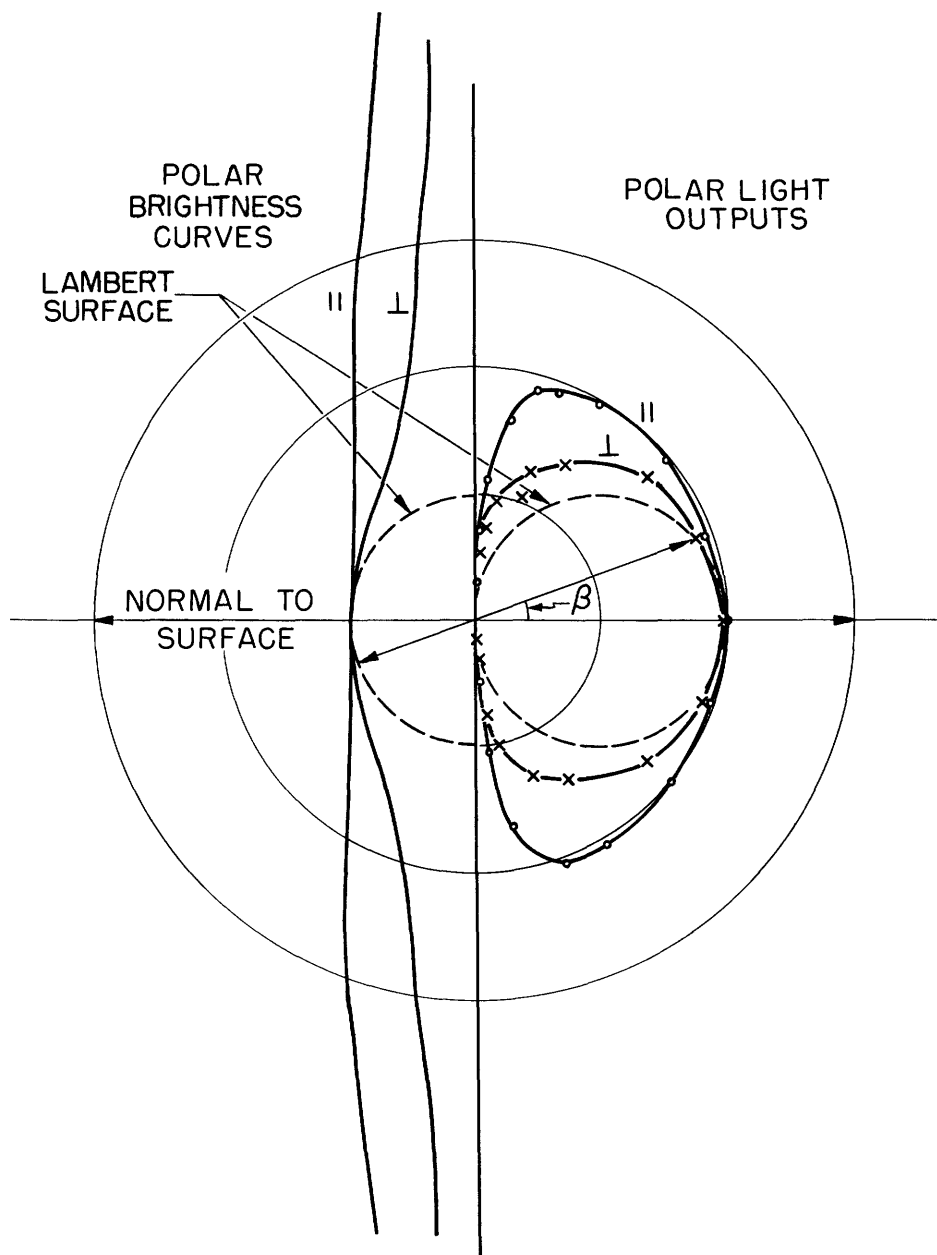


Fig. 10. Polar plots of surface brightness and total light output from a platinum-plate electrode, for different polarizations. (Standard solution,  $E = 0.9$  vdc.)



light of the correct polarization. The photocell and polarizer are located at the focus of a field lens that is sufficiently large to include the hydrofoil. The hydrofoil is viewed by means of this assembly from the direction that minimized the total area of severely inclined surfaces. The light intensity so measured provides an estimate of the integrated surface brightness of one half of the hydrofoil; viewed normal to a plane of symmetry it will indicate, in one measurement, the total surface integral of brightness, that is, the total light output. With conventional means this measurement would require more elaborate equipment, such as a completely transparent flow chamber.

### III. ILLUMINATION OF TRAILS AND WAKES

Using the same electrodes and solution as before, we have only to increase the applied voltage to obtain an entirely new visualization of the flow pattern. This effect is shown in Fig. 11 for a cylinder. Here we are generating at the boundary layer a glowing substance that is washed away by the fluid and passed downstream into the wake. The glow decays only gradually with time and distance. The glow produced is quite bright, more so than the boundary-layer display, a fortunate situation since the velocities of the parcels of fluid illuminated here are considerably greater than the velocities of the corresponding disturbances at the boundary layer. The difficulties in photographing these two presentations are approximately equal. For the photograph of Fig. 11 we have used our standard solution; some increase in the length of the trails is possible, however, if one uses a slightly less alkaline mixture.

Figure 12 illustrates the flow past a delta-wing airfoil at moderate Reynolds numbers for an angle of attack of approximately  $25^\circ$ , with both electrochemiluminescent techniques used. These two presentations complement each other. The exposure for the photograph of the wake was  $f3.5$  and  $1/100$  sec, with forced development to ASA 2000.

A disadvantage of the aqueous solution appears at low Reynolds numbers; the glowing catalyst generated at the boundary layer does not readily dissolve into the slowly moving fluid stream, but instead rises to the surface. If one uses a methanolic solution, this difficulty is considerably lessened because of the increased solubility of the catalyst generated at the electrode. The methanolic solution that we recommend is very similar in composition to the aqueous solution and uses tetramethylammonium chloride and hydroxide (each added in the same normality as in the aqueous solution). These reagents were chosen because of their more favorable solubility characteristics. The recommended concentration of luminol is also the same; we suggest adding twice the amount of  $H_2O_2$ , or 0.03 per cent, although this is not critical.

Another advantage of the methanolic solution for the display of trails and wakes is that we can vary the mean length of the trail over a wide range by controlling the pH. The more alkaline the solution, the shorter the trail—the total amount of light liberated appears to remain very nearly constant. This improved flexibility of operation is explained in part by the greater solubility of luminol in methanol; the luminol remains dissolved even if the solution is acidified to the point at which the chemiluminescence is completely inhibited.

We used such a methanolic solution to photograph the von Kármán trails generated by a cylinder moving in an arc, which are shown in Fig. 13. We are here looking from below, in line with the axis of the cylinder. Since it was undesirable to have any movement of the vortex street relative to the camera during the 0.2-sec exposure required for this photograph, we applied a small amount of counterrotation to the shallow cylindrical dish containing the fluid; this counterrotation compensated for the forward



Fig. 11. Cylinder discharging luminous trail, viewed from somewhat behind center.

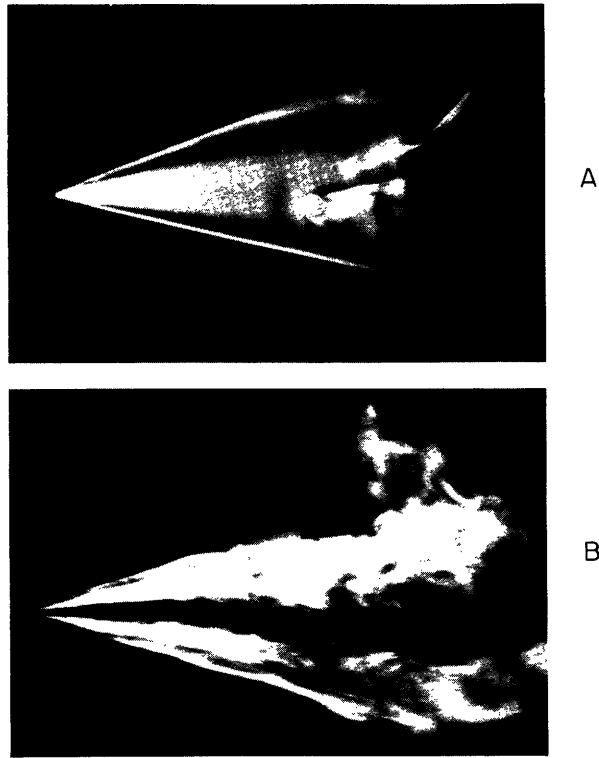


Fig. 12. Flow past delta-wing electrode, showing (a) boundary-layer display, and (b) luminous trail.



Fig. 13. Von Kármán trail generated by cylinder moving in a circular arc.

component of the vortices and for the slight motion otherwise imparted to the fluid by drag of the cylinder.

The ranges of application of the aqueous and methanolic solutions appear to complement one another. For high Reynolds numbers we chose the aqueous solution because of its greater light output. For low Reynolds numbers the methanolic solution produces satisfactory light output and is preferred because of its freedom from both bubbling and buoyancy effects. It is, of course, entirely possible that a solution can be compounded which has the advantage of both mixtures.

#### IV. SUMMARY

We have described in detail the technique by which electrochemiluminescence can be used to display the flow at the boundary layer of an electrode. The resulting surface-glow pattern is easily photographed; various states of flow about objects of simple shape have been illustrated. One can readily distinguish laminar from turbulent flows; also clearly visible are lines of flow separation and vortices.

The analogy between mass and heat transfers may provide us with an interpretation of these boundary-layer flow patterns; the intensity of glow is to be correlated with the local Nusselt number that would obtain in the comparable heat-transfer situation. Evidence was given to show that the surface brightness of the glow is, in fact, determined by the rate of mass transfer.

The electrochemiluminescent process was operated successfully with a number of nonaqueous solvents. Those having greater viscosity than water are of limited interest. However, those with reduced viscosity and Schmidt numbers are promising, since they require less power for operation at a given Reynolds number, and because, with their use, we may extend the range of applicability of the heat-transfer analogy.

An interesting characteristic of the electrochemiluminescent glow is the polar-brightness curve, which, experiments show, is highly non-Lambertian with pronounced polarization effects. Such measurements provide indirect evidence that the glow is generated very near the surface of the anode, that is, well inside the laminar sublayer. These measurements are relevant to the interpretation of the flow patterns, since they show that the apparent brightness of surfaces inclined to the direction of view is exaggerated.

The primary feature of the electrochemiluminescent boundary-layer display is that it gives a great deal of information concerning the state of flow at every point on the surface of a hydrofoil with no apparent disturbance to the flow situation. All flow phenomena that affect the mass- and heat-transfer coefficients can be expected to influence this presentation.

Altering the applied voltage changes radically the character of the display. With increased voltage, the glow extends into the solution and reveals the trail or wake. A methanolic solution is particularly useful here, since by altering the pH we can control the lifetime of the trail and its extension downstream. Using this second technique, we can study the von Kármán trail, or vortex street, caused by passage of cylinders through the solution.

## APPENDIX

### CALCULATION OF EXPOSURE FOR BOUNDARY-LAYER PHOTOGRAPHS

It is a well-known fact that the quality of a photograph depends considerably on the amount of light available; increased illumination permits the use of finer grain films, larger film size, and so forth. We have illustrated here the quality that is possible with modern, high-speed photographic materials used to photograph the flow patterns past hydrofoils of a few inches extent at moderate Reynolds numbers. It is reasonable to inquire as to the photographic exposure situation that will obtain at Reynolds numbers very much greater than we have considered, and also to study the effect, if any, of varying the scale factor,  $\lambda$ , that is assumed to control the dimensions of our modelling system.

Photographic exposure is determined by three factors: the surface brightness of the flow pattern, the shutter time, and the lens aperture setting (or "f" value). The variations of each of these parameters and of the total exposure with changes in the scale factor,  $\lambda$ , (for constant  $Re$ ) and with changes in  $Re$  (for constant  $\lambda$ ) are given in Table III. In this calculation we have considered two limiting cases: (a) the lens is set at maximum aperture, and (b) the setting of the lens aperture is governed by depth-of-field considerations.<sup>10</sup> The shutter times are determined on the basis of equal degrees of blurring of the image. Thus, for example, doubling the size of the hydrofoil with the Reynolds number held constant means that the fluid velocity will be halved; the time required for a disturbance at the boundary layer to move a given fractional distance along the hydrofoil will thus be increased by a factor of 4, and a shutter time

Table III. Dimensional analysis of exposure for boundary-layer photographs.

Quantity	Symbol	$\lambda$ Dependence (constant $Re$ )	$Re$ Dependence (constant $\lambda$ )
1. Size of hydrofoil	$L$	$\lambda^1$	$Re^0$
2. Fluid stream velocity	$v$	$\lambda^{-1}$	$Re^1$
3. Shutter Opening	$t = k \cdot L/v$	$\lambda^2$	$Re^{-1}$
4. Surface Brightness	$I$	$\lambda^{-1}$	$Re^{1/2}$
5. Relative Aperture (equal blurring)	$f$	$\lambda^{-1}$	$Re^0$
6. Exposure (a) (Maximum Aperture)	$t \cdot I$	$\lambda^1$	$Re^{-1/2}$
7. Exposure (b) (Aperture limited by depth of field)	$t \cdot I/f^2$	$\lambda^3$	$Re^{-1/2}$
8. Voltage drop in solution	$E$	$\lambda^0$	$Re^{1/2}$

four times longer will give the same degree of blurring. The "f" values are similarly calculated to give equal defocussing of those parts of the test object farthest removed from the image plane. Our calculations showing the dependence of exposures on Reynolds number should be regarded as tentative, since better information is needed on two points: our assumption that the shutter time varies with  $Re^{-1}$  (we do not know how the velocities of the disturbances at the boundary layer vary with fluid-stream velocity); and the criterion of equal blurring, since at higher Reynolds numbers the detail of the turbulent-wake structure may require finer photographic resolution.

These calculations indicate that the exposure situation will certainly be more favorable for large test objects than for small, the exposure varying with the scale factor as  $\lambda$  or  $\lambda^3$ , for maximal and depth-of-field limited aperture settings, respectively. It is further indicated that the exposure situation will be less favorable at large Reynolds numbers, although the exact dependence is uncertain. Together, these results suggest that if we wish to obtain good pictures of boundary-layer flow phenomena at very high Reynolds numbers, we may have to employ a larger and much more powerful flow chamber, since overcoming the unfavorable effects of the increased Reynolds number will require the use of a larger scale factor.

In the last row of Table III we give the voltage drop in the solution, which is measured from a hypothetical point at infinity to a point near the surface of the hydrofoil. We assume here that the surface density of current varies as the brightness. It is seen that this potential drop is independent of the scale factor and varies only slowly with Reynolds number. As we have stated, this voltage drop is not troublesome in the present experiments; if it should be significant at a much higher Reynolds number the concentration of peroxide could be reduced so as to decrease the current requirements.



### Acknowledgment

The authors wish to thank Miss Emma M. Duchane for her bibliographic research and for her many helpful suggestions concerning the experiments. We also wish to thank A. S. Richardson, Jr. and E. M. Christianson of the Department of Aeronautics, M. I. T., for supplying us with the airfoil section and for their helpful discussions. Thanks are extended to Professor W. Prichard Jones of the same department for suggesting the delta-wing experiment. We are also grateful to Professor A. H. Shapiro of the Department of Mechanical Engineering, M. I. T., for his interest in this work.

Mr. Bradford Howland is now a Staff Member of Lincoln Laboratory of the Massachusetts Institute of Technology.

## References

1. E. N. Harvey, J. Phys. Chem. 33, 1456-1459 (1929).
2. E. N. Harvey, Living Light (Princeton University Press, Princeton, N. J., 1940).
3. R. S. Anderson, Ann. N.Y. Acad. Sci. 49, 337 (1948).
4. D. N. Staicopoulos, Rev. Sci. Instr. 33, 176-178 (1961).
5. N. P. Campbell and I. A. Pless, Rev. Sci. Instr. 27, 875 (1956).
6. D. A. Frank-Kamenetskii, Diffusion and Heat Exchange in Chemical Kinetics (Princeton University Press, Princeton, N. J., 1955).
7. W. H. McAdams, Heat Transmission (McGraw-Hill Book Company, Inc., New York, 1954).
8. R. E. Eckert and E. Soehngen, Trans. Am. Soc. Mech. Engrs. 74, 343 (1952).
9. L. O. M. Von Rohr, Die Binokularen Instrumente (Springer Verlag, Berlin, 1920).
10. R. Kingslake, Lenses in Photography (Garden City Books, Garden City, N.Y., 1951).